Relativistic and nonrelativistic distorted-wave impulse approximation descriptions of the ^{208}Pb$(p, 2p)^{207}$Tl knockout reaction at medium incident energy

A. A. Cowley and G. C. Hillhouse

Department of Physics, University of Stellenbosch, Private Bag X1, Matieland, 7602, South Africa

Analyzing power and cross section energy distributions of protons knocked out in the reaction ^{208}Pb$(p, 2p)^{207}$Tl at an incident energy of 200 MeV are investigated in the framework of the distorted-wave impulse approximation. Non-relativistic as well as relativistic formulations are considered and compared. The influence of variations introduced by different implementations of the same basic theory is investigated.

1. Introduction

The need for a relativistic theory based on a Dirac description for the formulation of knockout reactions at moderate incident energies, as opposed to the more frequently-used nonrelativistic Schrödinger approach, is often considered. Whereas the proper relativistic treatment of the kinematical quantities is not in dispute, the evidence for a specific preference is otherwise not clear at all. In fact, Amos [1] has investigated the elastic scattering of protons up to fairly high incident energies and he finds that the predictive ability of cross section and analyzing power angular distributions are very similar for Dirac- and Schrödinger based formulations. Thus, in evaluating the significance of observed differences found between relativistic- and nonrelativistic theoretical results for other reaction types under certain kinematical conditions, one needs to ensure that these are not merely ascribable to sensitivities to the specific implementation of the formulations.

A detailed comparison between the nonrelativistic distorted wave impulse approximation (NDWIA) and the relativistic (RDWIA) equivalent is presented here. Predictions of analyzing power and cross section energy distributions of the reaction ^{208}Pb$(p, 2p)^{207}$Tl is investigated, and the sensitivity of the results to various ingredients that enter into the formulations in different ways, is studied. Accounts which concentrate mainly on either the NDWIA [2] or the RDWIA [3] have been published elsewhere. However, this review attempts to evaluate the results in a unified context and it expands the interpretation of the comparison.

One would expect that for such a heavy target nucleus as ^{208}Pb, for which distortion effects are severe, nominally equivalent optical potentials used to generate distorted waves would have a large influence on the values predicted for experimental observables. Surprisingly, it is found that both formulations are less sensitive to uncertainties in the optical potential parameters, as well as to uncertainties in other input quantities which need to be adopted from other type of experimental or theoretical reaction studies. The influence of the uncertainty of the relevant input ingredients where a direct correspondence can be established, is qualitatively similar in both types of theories.

We find that the RDWIA is able to give a reasonable reproduction of the analyzing power energy sharing distribution of knockout to the ground state, as well as to excited states of the final nucleus. The NDWIA calculations are only successful for the highest excitation. For cross section energy sharing distributions, of course, there are no significant systematic differences.

Although it is tempting to explain these results in terms of a fundamental superiority of the relativistic formulation, the fact that we are dealing with relatively moderate incident energy suggests that other reasons should be explored.

2. Theory

We write the general exclusive $(p, 2p)$ reaction as $A(a, a'b)C$. Thus an incident proton, a, knocks out a bound proton, b, from a specific orbital in the target nucleus, A, resulting in three particles in the final state, namely the recoil residual nucleus, C, and two outgoing protons, a' and b, which are detected in coincidence at coplanar laboratory scattering angles, $\theta_{a'}$ and θ_b, respectively. All kinematic quantities are completely determined by specifying the rest masses (m_i) of particles, where i = (a, A, a', b, C), the laboratory kinetic energy (T_a) of incident particle a, the laboratory kinetic energy ($T_{a'}$) of scattered particle a', the laboratory scattering angles $\theta_{a'}$ and θ_b, and also the binding energy of the proton that is to be knocked out of the target nucleus.

We present the theory in a very simplistic form only to illustrate the salient features and to indicate the considerations which apply to its implementation. Of course, full details are available in the references which are provided.

2.1 Nonrelativistic formulation

The nonrelativistic analysis was performed in terms of the DWIA formalism [4, 5]. For an interaction without a spin-orbit component, the differential cross section for the knockout reaction, which involves a bound proton that has a total angular momentum J and orbital angular momentum L, is given by

$$\frac{d^3\sigma}{d\Omega_{a'} d\Omega_b dT_{a'}} = F_K \; S_{LJ} \; \frac{d\sigma}{d\Omega}\bigg|_{a-b} \sum_{\Lambda} |T_{BA}^{\alpha L \Lambda}|^2 \; , \tag{1}$$

where F_K is a kinematic factor, $\frac{d\sigma}{d\Omega}|_{a-b}$ is a half-off-shell two-body a-b cross section, and S_{LJ} is the cluster spectroscopic factor for specific L (projection Λ) and J. The expression $\sum_\Lambda |T^{\alpha L\Lambda}_{BA}|^2$ is referred to as the distorted momentum distribution, where α represents additional quantum numbers.

Although spin-orbit interactions can clearly not be ignored in the present case, this simplified expression for the differential cross section nevertheless provides insight into the structure of the physical quantities that need to be evaluated in the case of polarized proton projectiles. For example, the full expression no longer factorizes when spin-orbit interactions are included, thus the half-off-shell two-body cross section does not appear simply as a multiplicative factor.

However, it remains a convenient approximation to replace the two-body amplitudes with those that describe the experimental free $a-b$ cross section values, which are fully on-shell. Two prescriptions may be used for this procedure: In the initial energy prescription (IEP) the scattering is assumed to occur with the relative energy of the projectile and the bound particle, while in the final energy prescription (FEP) the relative energy of the emitted particles a and b is assumed for this purpose. At the incident energy at which the present study was performed, the choice of prescription is not important.

2.2 Relativistic formulation

Although we will present results of the relativistic formulation in both finite range (FR) and zero range (ZR), for simplicity we summarise only the latter approximation. Full details are available in, for example, Ref. [3].

For a zero range approximation to the DWIA, the relativistic distorted wave transition matrix element is given by

$$\begin{aligned} T_{LJM_J}(s_a, s_{a'}, s_b) \;\; = \;\; & \int d\vec{r}\,[\,\bar{\psi}^{(-)}(\vec{r}, \vec{k}_{a'C}, s_{a'}) \otimes \bar{\psi}^{(-)}(\vec{r}, \vec{k}_{bC}, s_b)\,] \\ & \times \hat{t}_{NN}(T^{\ell\mathrm{ab}}_{\mathrm{eff}}, \theta^{\mathrm{cm}}_{\mathrm{eff}})[\,\psi^{(+)}(\vec{r}, \vec{k}_{aA}, s_a) \otimes \phi^B_{LJM_J}(\vec{r}\,)\,] \end{aligned} \tag{2}$$

where $T^{\ell\mathrm{ab}}_{\mathrm{eff}}$ and $\theta^{\mathrm{cm}}_{\mathrm{eff}}$ represent the effective two-body laboratory kinetic energy and effective center-of-mass scattering angles, respectively, and $\otimes$ denotes the kronecker product. The four-component scattering wave functions, $\psi(\vec{r}, \vec{k}_i, s_i)$, are solutions to the fixed-energy Dirac equation with spherical scalar and time-like vector nuclear optical potentials: $\psi^{(+)}(\vec{r}, \vec{k}_{aA}, s_a)$ is the relativistic scattering wave function of the incident particle, a, with outgoing boundary conditions [indicated by the superscript $(+)$], where $\vec{k}_{aA}$ is the momentum of particle a in the (a + A) center-of-mass system, and s_a is the spin projection of particle a with respect to $\vec{k}_{aA}$ as the $\hat{z}$-quantization axis; $\bar{\psi}^{(-)}(\vec{r}, \vec{k}_{jC}, s_j)$ is the adjoint relativistic scattering wave function for particle j [j = (a', b)] with incoming boundary conditions [indicated by the superscript $(-)$], where $\vec{k}_{jC}$ is the momentum of particle j in the (j + C) center-of-mass system, and s_j is the spin projection of particle j with respect to $\vec{k}_{jC}$ as the $\hat{z}$-quantization axis. The bound state proton wave function, $\phi^B_{LJM_J}(\vec{r}\,)$, with single-particle quantum numbers L, J, and M_J, is obtained via selfconsistent solution to the Dirac-Hartree field equations of quantum hadrodynamics [6].

In addition, we adopt the impulse approximation which assumes that the form of the NN scattering matrix in the nuclear medium is the same as that for free NN scattering: the NN scattering matrix, $\hat{t}_{NN}$, is parameterized in terms of five Lorentz invariants (scalar, pseudoscalar, vector, axial-vector, tensor), the so-called IA1 representation, which are directly related to the nonrelativistic Wolfenstein amplitudes. Note that the periodic nature of the three-dimensional integrand, given by Eq. (2), ensures numerical stability and rapid convergence.

2.3 Analyzing power

The spin observables of interest are denoted by $\mathrm{D}_{i'j}$ and are related to the probability that an incident beam of particles, a, with spin-polarization j induces a spin-polarization i' for the scattered beam of particles, a': the subscript $j = (0, \ell, n, s)$ is used to specify the polarization of the incident beam a along any of the orthogonal directions

$$\begin{aligned} \hat{\ell} &= \hat{z} = \hat{k}_{aA} \\ \hat{n} &= \hat{y} = \hat{k}_{a_A} \times \hat{k}_{a'C} \\ \hat{s} &= \hat{x} - \hat{n} \times \hat{\ell}, \end{aligned} \tag{3}$$

and the subscript $i' = (0, \ell', n', s')$ denotes the polarization of the scattered beam a' along any of the orthogonal directions:

$$\begin{aligned} \hat{\ell}' &= \hat{z}' = \hat{k}_{a'C} \\ \hat{n}' &= \hat{n} = \hat{y} \\ \hat{s}' &= \hat{x}' = \hat{n} \times \hat{\ell}' \,. \end{aligned} \tag{4}$$

The subscript $i' = j = 0$ is used to denote an unpolarized beam. With the above coordinate axes in the initial and final channels, the spin observables, $\mathrm{D}_{i'j}$, are defined by

$$\mathrm{D}_{i'j} = \frac{\mathrm{Tr}(T\sigma_j T^\dagger \sigma_{i'})}{\mathrm{Tr}(TT^\dagger)} \,, \tag{5}$$

where $\mathrm{D}_{n0} = P$ refers to the induced polarization, $\mathrm{D}_{0n} = A_y$ denotes the analyzing power, and the other polarization transfer observables of interest are D_{nn}, $\mathrm{D}_{s's}$, $\mathrm{D}_{\ell'\ell}$, $\mathrm{D}_{s'\ell}$, and $\mathrm{D}_{\ell's}$. The denominator of Eq. (5) is related to the unpolarized triple differential cross section, that is,

$$\frac{d^3\sigma}{dT_{a'}\, d\Omega_{a'}\, d\Omega_b} \propto \mathrm{Tr}(T\,T^\dagger) \,. \tag{6}$$

In Eq. (5), the symbols $\sigma_{i'}$ and σ_j denote the usual 2×2 Pauli spin matrices, namely,

$$\begin{aligned} \sigma_0 &= \begin{pmatrix} 1 & 0 \\ 0 & 1 \end{pmatrix} \\ \sigma_{s'} &= \sigma_s = \sigma_x = \begin{pmatrix} 0 & 1 \\ 1 & 0 \end{pmatrix} \\ \sigma_n &= \sigma_y = \begin{pmatrix} 0 & -i \\ i & 0 \end{pmatrix} \\ \sigma_{\ell'} &= \sigma_\ell = \sigma_z = \begin{pmatrix} 1 & 0 \\ 0 & -1 \end{pmatrix} \end{aligned} \tag{7}$$

and the 2×2 matrix T is given by

$$T = \begin{pmatrix} T_{LJ}^{s_a=+\frac{1}{2}, s_{a'}=+\frac{1}{2}} & T_{LJ}^{s_a=-\frac{1}{2}, s_{a'}=+\frac{1}{2}} \\ T_{LJ}^{s_a=+\frac{1}{2}, s_{a'}=-\frac{1}{2}} & T_{LJ}^{s_a=-\frac{1}{2}, s_{a'}=-\frac{1}{2}} \end{pmatrix} \tag{8}$$

where $s_a = \pm\frac{1}{2}$ and $s_{a'} = \pm\frac{1}{2}$ refer to the spin projections of particles a and a' along the $\hat{z}$ and $\hat{z}'$ axes, defined in Eqs. (3) and (4), respectively; the matrix $T_{LJ}^{s_a, s_{a'}}$ is related to the relativistic $(p, 2p)$ transition matrix element $T_{LJM_J}(s_a, s_{a'}, s_b)$, defined in Eq. (2), via

$$T_{LJ}^{s_a, s_{a'}} = \sum_{M_J, s_b} T_{LJM_J}(s_a, s_{a'}, s_b) \, . \tag{9}$$

3. Comparison of non-relativistic distorted-wave impulse approximation (NDWIA) results with experimental data

Theoretical cross section and analyzing power energy-sharing distributions predicted by the NDWIA were compared with experimental data for the reaction ^{208}Pb($\vec{p}$,2p)^{207}Tl at an incident energy of 200 MeV. Calculations were performed with the code THREEDEE of Chant [7].

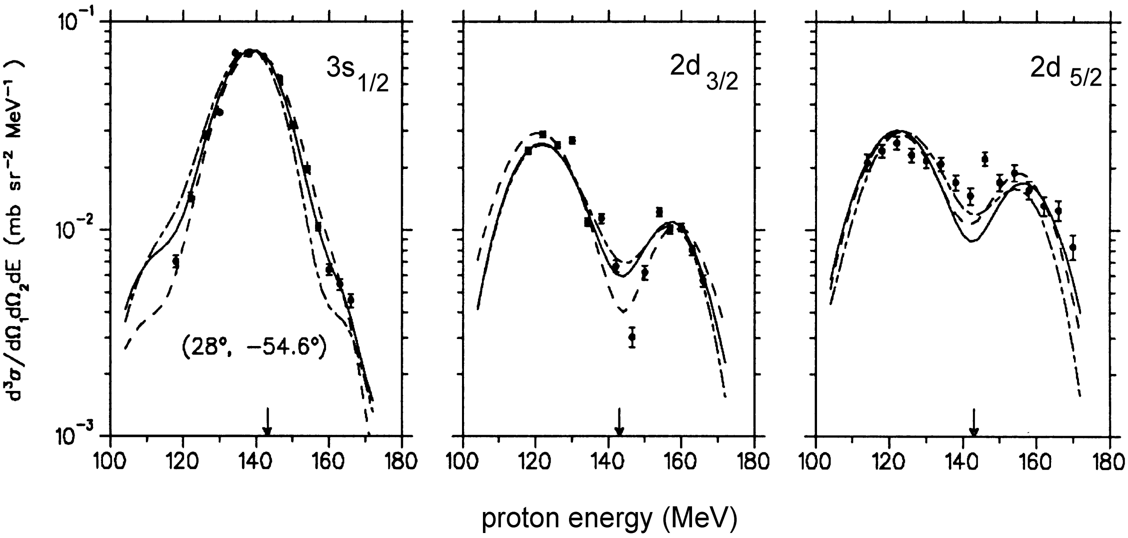

Fig. 1 Energy-sharing cross section distributions for the ^{208}Pb(p,2p)^{207}Tl reaction at 200 MeV, with coincident protons observed at coplanar angles of 28° and 55° on the opposite side of the beam (as implied by the negative sign of the second angle). Results are shown for knockout of protons from three shell model orbitals as a function of the energy of the proton observed at 28°. The curves represent NDWIA predictions for the free nucleon-nucleon interaction and distorting optical model potential parameter sets of Schwandt [8] (solid line), Nadasen [9] (dashed line) and Hama [10] (dot-dashed line). Arrows indicate the position of minimum (essentially zero) recoil.

Ingredients of the theory, which are derived from investigations which are unrelated to this study, which could possibly affect the predicted distributions, are the wave function of the bound proton which enters into the expression for the distorted momentum distribution, the optical potentials parameters used to generate distorted waves, and the influence of nuclear-matter density-dependence of the nucleon-nucleon interaction.

As mentioned by Miller *et al.* [11], the values of potential-parameters that are used to calculate the bound-state wave function, are constrained well by electron scattering data. These were taken from the work of Mahaux and Sartor [12]. The results were found to be insensitive to other choices for the bound state.

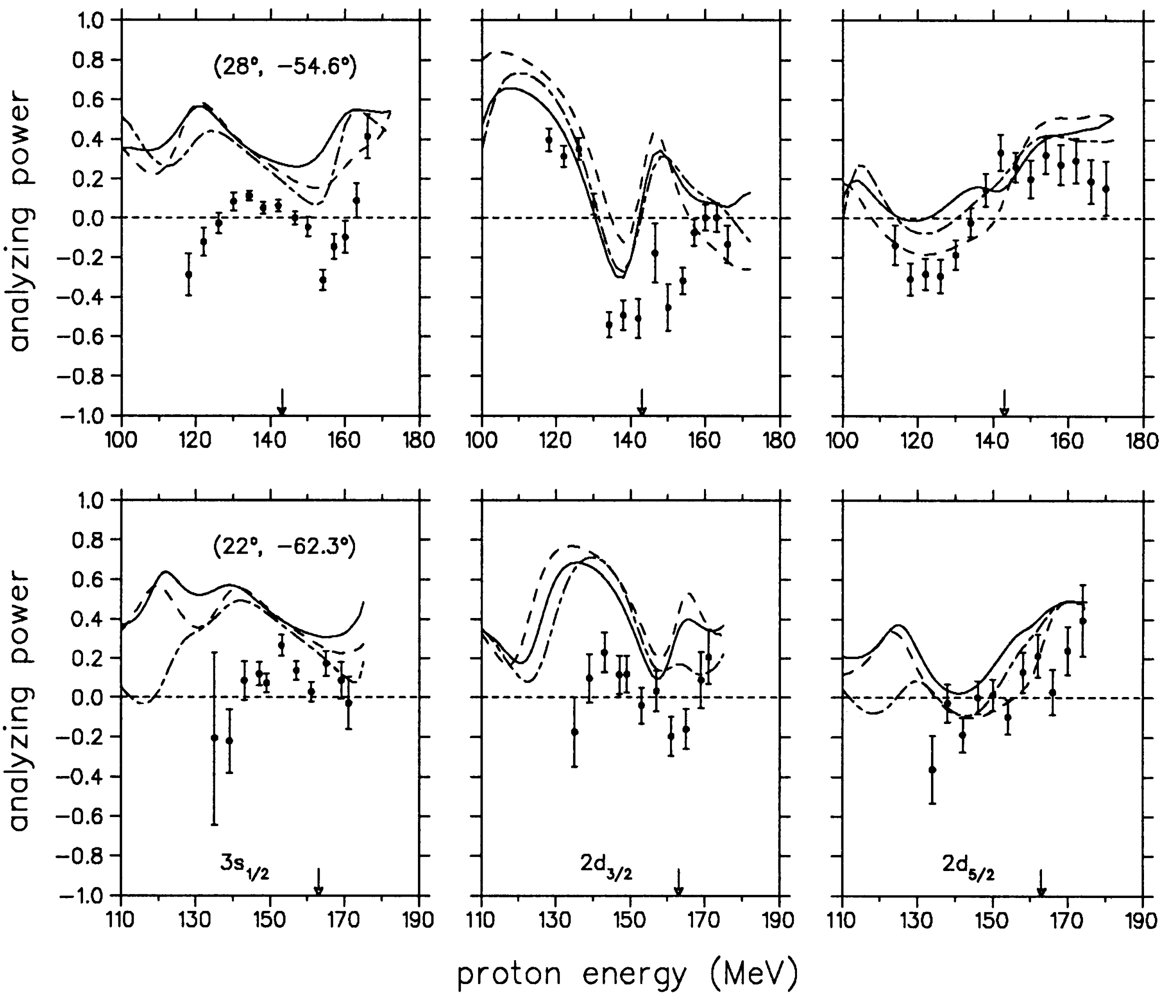

Fig. 2 Energy-sharing analyzing power distributions for the ^{208}Pb(p,2p)^{207}Tl reaction at 200 MeV. Other details are as indicated in Fig. 1, with the three curves representing predictions of the different optical potentials adopted, as identified in Fig. 1.

Different sets of global optical potentials to generate distorted waves were investigated. Representative results are shown in Figs. 1 and 2 for three sets. These include a set generated by a Schrödinger equivalent reduction of the global Dirac analysis of Hama *et al.* [10], a set from the work of Schwandt *et al.* [8], and the parameters of Nadasen *et al.* [9].

We find that the results are relatively insensitive to the distorting potentials with regard to cross section energy-sharing distributions, as shown in Fig. 1. The agreement between the predictions and the experimental values is reasonable in all cases investigated, with spectroscopic values which are in fair agreement with expectation. However, the analyzing power energy-sharing distributions shown in Fig. 2 display a larger difference, and especially for knockout of $3s_{1/2}$ protons, none of the theories succeeds in reproducing the experimental distributions.

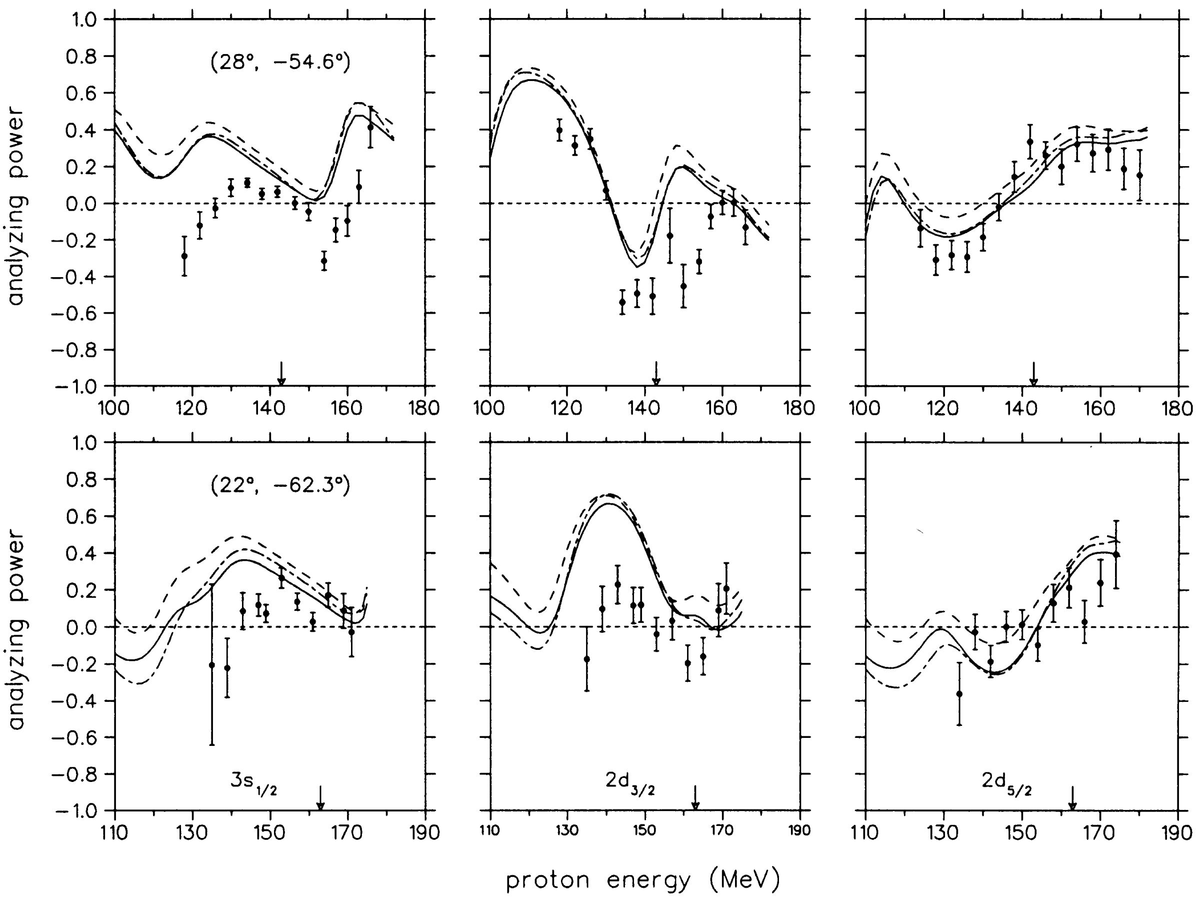

Fig. 3 Energy-sharing analyzing power distributions for the ^{208}Pb(p,2p)^{207}Tl reaction at 200 MeV. Theoretical distributions are presented for the free nucleon-nucleon interaction (dashed line), the Kelly [14] density dependent interaction (solid line) and the Horowitz and Iqbal [13] formulation.

The density dependence of the $a - b$ two-body interaction was explored in two ways. The first was to introduce modifications to the two-body t matrix in a local density approximation according to the method of Horowitz and Iqbal [13]. The second, alternative approach, was to use an empirical density dependence as found by Kelly *et al.* (See Ref. [14]).

As can be seen in Fig. 3, the alternative treatments of the density dependence improve the agreement with the experimental analyzing power distributions to roughly the same extent. Not shown are the cross-section distributions, which are affected neglibly by the introduction of a density dependence.

Clearly the inclusion of a density dependence improves the agreement with the data in all cases, however only knockout from the $2d_{5/2}$-state is reproduced satisfactorally. The distribution of the $3s_{1/2}$ state, especially, is described rather badly.

4. Results obtained with the relativistic distorted-wave impulse approximation (RDWIA)

Analyzing power energy distributions predicted by the zero-range RDWIA are shown in Fig. 4, without medium modifications to the nucleon-nucleon interaction. In spite of the neglect of finite-range effects, the theory gives an excellent reproduction of the experimental distributions. Although results for different global Dirac optical potential parameter sets are not shown, they were found to be insensitive to the exact choice of parameter set, with differences in the results being of the order of the experimental error bars. (Again, as with the NDWIA, the predicted cross section distributions, which are not displayed, are in acceptable agreement with the experimental data). Comparison with the NDWIA results of Fig. 2 clearly shows the dramatic superiority of the RDWIA, especially with respect to the $3s_{1/2}$ ground state reaction.

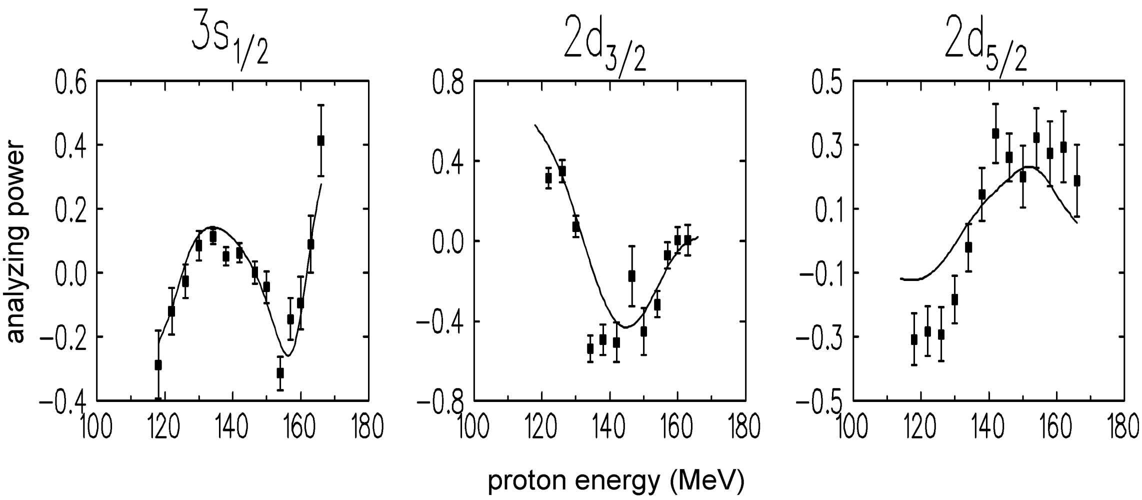

Fig. 4 Energy-sharing analyzing power distributions for the ^{208}Pb$(p,2p)^{207}$Tl reaction at 200 MeV, with coincident protons observed at coplanar angles of 28° and -55°. Other details are as indicated in Fig. 1. The theoretical curves represent zero-range RDWIA calculations.

If finite-range effects are included in the calculations, the agreement with the experimental analyzing power distributions deteriorate somewhat, as shown in Fig. 5. However, when in addition we include medium modifications of the nucleon-nucleon interaction, the results improve, as expected. In fact, with the medium-modified coupling constants and meson masses reduced by a very modest amount of 10%, we appear to obtain the best agreement with the experimental distributions.

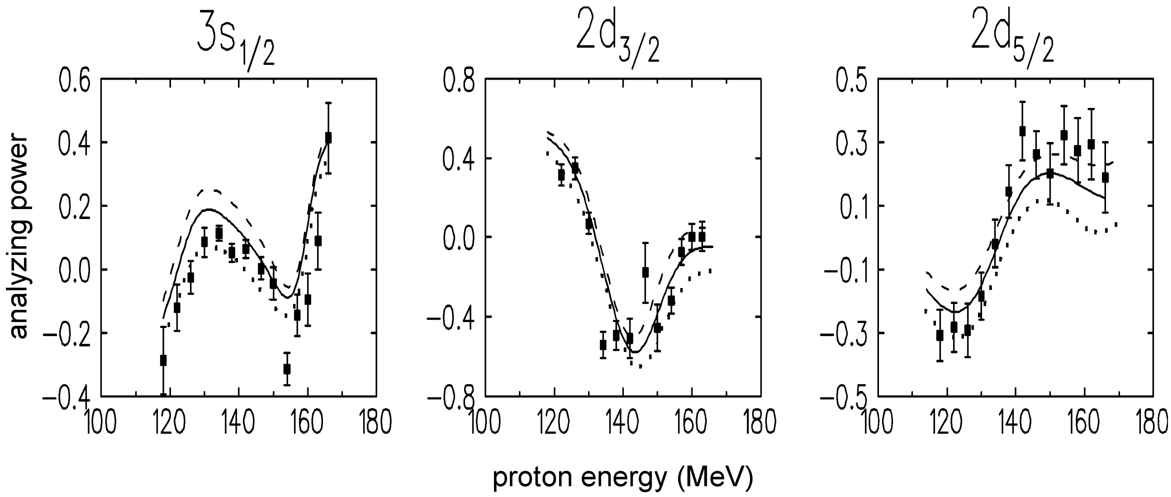

Fig. 5 Energy-sharing analyzing power distributions for the ^{208}Pb(p,2p)^{207}Tl reaction at 200 MeV, with coincident protons observed at coplanar angles of 28° and -55°. Other details are as indicated in Fig. 1. The theoretical curves represent finite-range RDWIA calculations with medium-modification excluded (dashed line), included with a 10% reduction (solid curves) and 20% reduction (dotted line) of the medium-modified coupling constants and meson masses.

5. Summary and conclusions

This work focuses on a comparison between relativistic and nonrelativistic distorted wave descriptions for exclusive proton knockout from the $3s_{1/2}$, $2d_{3/2}$ and $2d_{5/2}$ states in ^{208}Pb, at an incident energy of 200 MeV, and for coincident coplanar scattering angles $(28.0°, -54.6°)$. In spite of exhaustive corrections to the nonrelativistic model it fails to account for the analyzing power for $3s_{1/2}$- and $2d_{3/2}$-knockout. Such a systematic analysis was also performed with the finite as well as zero range RDWIA, with density-dependent corrections to the NN interaction taken into account.

In this paper we have demonstrated the superiority of the relativistic Dirac-equation, as compared to the nonrelativistic Schrödinger equation, for the description of the exclusive $(\vec{p}, 2p)$ analyzing powers, for proton-knockout from ^{208}Pb at 200 MeV, within the context of the DWIA. This result is somewhat surprising, based on the relatively low incident energy and the suggestion from elastic scattering investigations which imply that the two approaches should not differ in practice.

Both relativistic ZR and FR approximations to the DWIA provide an excellent description of the analyzing power data. On one hand, the relativistic ZR predictions suggest that the scattering matrix for NN scattering in the nuclear medium is adequately represented by the corresponding matrix for free NN scattering and, hence it is not necessary to consider nuclear medium modifications to the NN interaction. On the other hand, the relativistic FR results suggest that a modest 10% reduction of meson-coupling constants and meson masses by the nuclear medium is needed for providing a consistent description of the $3s_{1/2}$, $2d_{3/2}$ and $2d_{5/2}$ analyzing powers. In order to extract more conclusive information regarding the influence of the nuclear medium on the properties of the strong interaction, it may be necessary to study complete sets of polarization transfer observables for the exclusive knockout of protons from deeper-lying states in a variety of nuclei.

This material is based upon work supported by the National Research Foundation under Grant numbers: GUN 2058507, 2053786, 2053773.

References

[1] K. Amos, private communication.

[2] R. Neveling *et al.*, Phys. Rev. C **66** (2002) 034602.

[3] G. C. Hillhouse, J. Mano, A. A. Cowley and R. Neveling, Phys Rev (2003) in press.

[4] N. S. Chant and P. G. Roos, Phys. Rev. C **15** (1977) 57.

[5] N. S. Chant and P. G. Roos, Phys. Rev. C **27** (1983) 1060.

[6] C. J. Horowitz and B. D. Serot, Nucl. Phys. **A368** (1981) 503 .

[7] N. S. Chant and P. G. Roos, THREEDEE code, University of Maryland (1998) (unpublished)

[8] P. Schwandt *et al.*, Phys. Rev. C **26** (1982) 55.

[9] A. Nadasen *et al.*, Phys. Rev. C **23** (1981) 1023.

[10] S. Hama *et al*., Phys. Rev. C **41** (1990) 2737.

[11] C. A. Miller *et al.*, Phys. Rev. C **57**(1998) 1756.

[12] C. Mahaux and R. Sartor, Nucl. Phys. A 481 (1988) 381.

[13] C. J. Horowitz and M. J. Iqbal, Phys. Rev. C **33** (1986) 2059.

[14] H. Seifert *et al.*, Phys. Rev. C **47** (1993) 1615, and references therein.